Hindawi
Journal of Nanomaterials
Volume 2022, Article ID 7490221, 16 pages
https://doi.org/10.1155/2022/7490221

Research Article

Biosynthesis of Silver Nanoparticles by Polysaccharide of *Leucaena leucocephala* Seeds and Their Anticancer, Antifungal Properties and as Preservative of Composite Milk Sample

Mohamed A. Taher[1], **Ebtihal Khojah**[2], **Mohamed Samir Darwish**[3], **Elsherbiny A. Elsherbiny**[4], **Asmaa A. Elawady**[3] and **Dawood H. Dawood**[1]

[1]*Agricultural Chemistry Department, Faculty of Agriculture, Mansoura University, Mansoura 35516, Egypt*
[2]*Department of Food Science and Nutrition, College of Science, Taif University, P.O. Box 11099, Taif 21944, Saudi Arabia*
[3]*Dairy Department, Faculty of Agriculture, Mansoura University, Mansoura 35516, Egypt*
[4]*Plant Pathology Department, Faculty of Agriculture, Mansoura University, Mansoura 35516, Egypt*

Correspondence should be addressed to Mohamed A. Taher; mohamedtaher@mans.edu.eg

Received 21 November 2021; Accepted 9 January 2022; Published 25 January 2022

Academic Editor: José Agustín Tapia Hernández

The AgNPs were synthesized using water-soluble polysaccharides extracted from the *Leucaena leucocephala* seeds. The UV-visible spectrum of the AgNPs showed a sharp absorption peak at 448 nm. The XRD analysis showed four major peaks of the crystalline AgNPs with planes of a face-centered cubic lattice of silver. The EDS spectrum showed a strong signal peak at ~3 keV. TEM and SEM observations showed the spherical shape of AgNPs with no particle agglomeration, and the size ranged from 8 to 20 nm. AgNPs were highly stable at -14.2 mV by zeta potential measurement. AgNPs showed significant anticancer activity against the cell lines of breast cancer, liver carcinoma, and colon carcinoma with the IC_{50} value of 22.5, 12.3, and 8.9 $\mu g\,mL^{-1}$, respectively. AgNPs at 900 $\mu g\,mL^{-1}$ exhibited considerable antifungal activity against ten fungal pathogens. Water-soluble polysaccharide has the ability to synthesize AgNPs keeping strong antitumor, antifungal activities. The AgNPs can slow down spoilage of composite milk samples at different temperatures. In addition, the accuracy of milk-IR-analyses was not affected by different concentrations of AgNPs.

1. Introduction

Nanoparticles are of great research attention as they have innovative optoelectronic, magnetic, and physicochemical features, affected by their various shape and size details [1]. Researchers are most interested in the biosynthesis of stable nanoparticles using green chemistry routes in which no xenobiotic or toxic compounds are used for environmental sustainability. Green synthesis of nanoparticles depends on natural reduction components commonly found in bacteria, fungi, yeast, actinomycetes, and plant extracts [1]. In a few recent years, the polysaccharide-mediated green synthesis of different metal nanoparticles had a voluminous role in nanobiotechnology [2]. Several examples are available of stable metal nanoparticles biosynthesis by polysaccharides which chiefly comprise gold, silver, zinc, and palladium nanoparticles.

Among zero-dimensional nanomaterials, silver nanoparticles (AgNPs) are one of the worthiest candidates for performant and unconventional applications, with enormous outcomes in pharmaceutical sciences, cosmetics, wound dressings, and anti-infective coatings, antimicrobial textiles, and food packages [3, 4]. The major role of AgNPs in medicine mostly depends on their exceptional and wide antimicrobial activity [3, 4]. On the other hand, the utilization of nanosilver for prolonging the shelf life of dairy products is not probable as the minimum inhibitory concentration of silver is at least 5 $mg\,L^{-1}$ in milk which was greater than the WHO-recommended maximum concentration of AgNPs (0.1 $mg\,L^{-1}$) [5]. However, to date, there are no data in

the literature that indicate the suitability of AgNPs as a potential substitute for chemical preservative agents of milk composite samples without any effect on the accuracy of infrared (IR) devices to tested samples.

The area of food and agriculture research takes benefit of wastes from agroindustrial and agricultural sources to give them an added value, thus avoiding pollution to the environment by minimizing burning or extreme accumulation [6]. In this context, *Leucaena leucocephala* (Lam.) is a tropical tree that grows in Egypt, perennial thornless, with a height of around 8 m, and belongs to the subfamily Mimosoideae and family Fabaceae with bulk volumes of solid wastes in the form of leaves, ripened fruits, pods, and seeds [7]. This tree is commonly used as organic fertilizer, timber, gum, fuel, forage, firewood, and raw mass for paper and pharmaceutical industries [8]. Moreover, the tree has different biomedical properties, including antiviral, antidiabetic, anti-inflammatory, anticancer, antithrombotic, anticoagulant, and immunostimulant properties [9, 10]. The seed gums of *L. leucocephala* are used for treating gastric tract diseases and well act as a laxative, while the whole seed has been used as a coffee substitute.

The galactomannan gum is the predominant constituent in the seeds of *L. leucocephala* with insignificant levels of tannins, organic acids, oils, and the amino acid of mimosine [11]. The viscous galactomannan obtained from the endosperm of *L. leucocephala* seeds is structured as linear chains of β-(1-4)-d-mannose units substituted by single α-d-galactose units at O-6. The galactose/mannose ratio of *Leucaena* gum is approximately 1 : 1.3, although the galactose/mannose ratio is variable between species, portions, or even fractions of *Leucaena* [12]. Recently, the different extracts of *L. leucocephala* have been used in developing metal-based nanoparticles such as copper, silver, and cadmium [13–15].

To our best knowledge, no documents have been directed on the use of polysaccharides of galactomannan precipitated from the seed wastes of *L. leucocephala* for developing silver nanoparticles. Therefore, the present study is aimed at (1) precipitating the crude polysaccharide of *L. leucocephala* seeds, (2) characterizing the chemical composition of the crude polysaccharide, (3) using the crude polysaccharide in the preparation of silver nanoparticles, (4) characterizing the synthesized AgNPs using polysaccharides of *L. leucocephala* seeds, (5) estimating the antitumor and antifungal activities of the biosynthesized AgNPs, (6) evaluating the preservative action of the AgNPs in composite milk samples, and (7) determining the influence of AgNPs on the accuracy of midinfrared milk component testing.

2. Materials and Methods

2.1. General. Absolute ethanol, silver nitrate ($AgNO_3$), methanol, petroleum ether (60-80°C), sulfuric acid, 3,5-dinitrosalicylic acid (DNS), Folin-Ciocalteu reagent, gallic acid, phenol crystal, and sodium carbonate (anhydrous) were purchased from Sigma (Sigma-Aldrich Chemicals, USA). The seeds of *L. leucocephala* were collected from Mansoura University Campus in Mansoura city. The plant materials were authenticated by a plant taxonomist at the Botany Department, Faculty of Science, Mansoura University, Egypt.

The fungal species of *Alternaria alternata* AUMC 10301, *Aspergillus flavus* AUMC 8965, *A. parasiticus* AUMC 8947, *Bipolaris hawaiiensis* AUMC 1120, *B. spicifera* AUMC 459, *Botrytis cinerea* AUMC 6095, *Cochliobolus cynodontis* AUMC 2393, *Fusarium oxysporum* AUMC 9704, *F. sambucinum* AUMC 1266, and *Penicillium digitatum* AUMC 2206 were obtained from Assiut University Mycological Centre (AUMC), Egypt. The bacterial strains of *Escherichia coli* MSD102, *Enterococcus faecalis* MSD23, *Lactobacillus delbrueckii* subsp. *bulgaricus* MSD231, and *Streptococcus thermophilus* AAE84 were obtained from the Laboratory of Dairy Microbiology at Dairy Department, Faculty of Agriculture, Mansoura University, Egypt.

2.2. Extraction of Crude Polysaccharides. The crude polysaccharide of *L. leucocephala* was extracted according to the protocol mentioned by Dawood et al. [16]. In detail, twenty grams of dry seeds powder were extracted with petroleum ether (40–60°C) for 6 h for removal of lipid materials. The pretreated dry powder was extracted three times each for 120 minutes with deionized water (water-solid material; $10 : 1\,mL\,g^{-1}$) at 70°C. The insoluble materials were detached by filtration, and the water-soluble solution was concentrated under a vacuum at 50°C. The precipitation process was then originated by the anhydrous ethanol addition to a final concentration of 75% (v/v) to the concentrated extract; the mixture was then kept for 24 h at 4°C, followed by centrifugation at $12000 \times g$ for 15 min, and then the resulting precipitate was dried by air-dried to afford crude polysaccharides named LLPs.

2.3. Quantitative Analysis of Reducing Sugar and Total Carbohydrates Concentration. The concentration of total carbohydrates was estimated by the phenol-sulfuric acid method previously written [17]. D-Glucose was used as a standard for calculating the total carbohydrate concentration. The determination of reducing sugar was carried out according to the Miller method [18]. The reducing sugar was subtracted from the total carbohydrate to calculate the total polysaccharide of LLPs.

2.4. Determination of Protein Content and Total Polyphenol Content. The protein content was determined by the Kjeldahl nitrogen determination method [19]. The content of total polyphenols content of the LLPs was determined according to Taher et al. [20]. It was expressed as a milligram of gallic acid equivalent per gram of LLPs (mg GAE/g).

2.5. Identification of LLP Components by Thin Layer Chromatography (TLC). The final residue of LLPs was dissolved in an appropriate volume of 40% methanol, and TLC was done using precoated silica gel GF 254 plates according to the details written by Mittal et al. [21]. Galactose (G) and mannose (M) were used as standards.

2.6. Nuclear Magnetic Resonance Spectroscopy. Nuclear magnetic resonance (NMR) spectra were obtained using a 400 MHz Bruker Avance III spectrometer with a 5 mm inverse

probe. The spectra were noted using a 1% (w/v) solution of LLPs in deuterium oxide (D_2O).

2.7. Synthesis of AgNPs. To synthesize AgNPs, 50 mg of LLPs was dissolved in 100 mL of distilled water and mixed with 200 mL of 0.1 mM $AgNO_3$, and the solution was stirred with a magnetic stirrer for 30 min at 60°C under constant stirring. Bioreduction occurs quickly as shown by a reddish-brown color after 36 h representing the AgNPs formation (AgNPs were regularly checked by visual assessment of the solution as well as by ultraviolet-visible spectroscopy), followed by repeated centrifugation at $12000 \times g$ for 20 min to collect AgNPs. The pellets were collected and dried [22].

2.8. Characterization of Biosynthesized AgNPs. The characterization of biosynthesized silver nanoparticles was determined by an ultraviolet-visible spectroscopy spectrophotometer (UV-2550, Shimadzu, Japan) with a spectral resolution of 1 nm over a wavelength ranging from 300 to 600 nm. For identification of the functional groups and chemical bonding in the silver nanoparticles, 300 mg of fine potassium bromide (KBr) was mixed with one milligram of each sample. The preparation of thin pellets was carried out using hydraulic pellet press, followed by subjecting to the Fourier-transform infrared spectrophotometer (FTIR) ranging between 500 and 4000 cm^{-1} at a resolution of 4 cm^{-1} (Bruker Vector 22).

The crystalline structure of the biosynthesized AgNPs was analyzed by the X-ray diffractometer (D8 Advance, Bruker, Germany) operating at 40 kV using Cu-Kα radiation with λ of 1.54 Å and scanning rate 0.1° in the 2θ range from 5° to 80°. The elemental composition of the AgNPs was identified by energy-dispersive spectroscopy (EDS) attached with scanning electron microscopy (JEOL JSM-6510LV) between 0 and 20 kV.

The morphology of the synthesized AgNPs was carried out with a JEOL JSM-6510LV scanning electron microscopy (SEM) operating at an electron accelerating voltage of 30 kV. A very small sample size was put on a carbon-coated copper grid. The film on the grid was then dried at room temperature before SEM analysis. The transmission electron microscopy (TEM, Model JEM 2100LV, JOEL, Japan) was used to analyze the size and shape of the AgNPs. A drop of biosynthesized AgNPs was put on the carbon-coated copper grid and then loaded onto a specimen holder before the sample observation. The stability of Ag nanoparticles was evaluated using the Zeta-Sizer Nano-ZS90 (Malvern Instruments Ltd., UK).

2.9. Antitumor Activity. The antitumor activity was conducted in vitro on liver carcinoma (HEPG-2), colon carcinoma (HCT-116), and breast cancer (MCF-7) cell lines (ATCC, Minnesota, USA) using the sulforhodamine B stain (SRB) assay [23].

In detail, the cells were cultured in RPMI-1640 medium enriched with 10% fetal bovine serum and 1% streptomycin/penicillin. Different concentrations of AgNPs and 5-fluorouracil (5-FU), as a reference drug (6.25, 12.5, 25, 50, and 100 $\mu g\,mL^{-1}$) were prepared in the culture medium. The cells were added to 96-well microtiter plates at the concentration of 3×10^3 cells per well in a 150 μL fresh medium and left for 24 h to attach to the plates. Then, 100 μL of 5-FU (positive control) and each AgNP concentration was added to every well except the control wells. After 48 h, the cells were fixed with 50 μL of ice-cold trichloroacetic acid (10% w/v), followed by incubation at 4°C for 1 h. The addition of 50 μL of SRB (0.4% w/v in 1% aqueous acetic acid) stained the TCA-fixed cells. The plates were incubated for 30 min at room temperature. The acetic acid (1% v/v) was used for washing the plates four times to remove the unbound, followed by drying. The bound SRB was solubilised by adding 200 μL of 10 mM Tris Base (pH 10.5) to each well and shaking for 5-10 min. The absorbance of microplates at 570 nm was determined by a 96-well plate reader. The percentage of cell viability inhibition was estimated in comparison to the control.

2.10. Antifungal Activity. The silver nanoparticles were individually tested against the previously mentioned ten fungal strains. A mycelial disk of each of the fungi (5 mm diameter) was placed in the center of each potato dextrose agar (PDA) plate (90 mm diameter) containing the final concentrations of AgNPs at 0 (control), 300, 500, 700, and 900 $\mu g\,mL^{-1}$. All plates were incubated at 25 ± 2°C until the growth in the control reached the edge of the plates. Each treatment was performed in triplicate, and the experiment was repeated twice. The inhibition of mycelial growth was calculated as follows: Mycelial growth Inhibition $(\%) = [(C - T)/C] \times 100$, where C (mm) and T (mm) are the mean growth diameter in the control and treatment, respectively [24].

2.11. Correlation between Log of Cell Numbers (CFU/mL) and Milk Acidification (pH). The spread plate method was carried out to determine the numbers of bacterial cells using MRS and M17 agar for *Lactobacillus delbrueckii* subsp. *bulgaricus* MSD231and *Streptococcus thermophilus* AAE84, respectively, at 42°C for 24 h, while using TSA for *Escherichia coli* MSD102 and *Enterococcus faecalis* MSD23 at 37°C for 24 h. Acidification of milk using the growth of the previously mentioned four bacterial strains was determined by a pH meter (Hanna Hi2210). A correlation between log values of cell numbers (CFU) and pH was performed by the TableCurve 2D software [5].

2.12. The Practical Parameters for the Assessment of AgNP Preserved Composite Milk Samples

2.12.1. Milk Samples and Preservation. Reconstituted milk was made from powder full cream milk obtained from a local market in Mansoura city, Egypt. The process for producing the reconstituted milk was carried out according to Braun, Ilberg, Blum, and Langowski [5]. The reconstituted milk was divided into 4 equal parts. The first, second, third, and fourth parts were individually inoculated with *Escherichia coli* MSD102, *Enterococcus faecalis* MSD23, *Lactobacillus delbrueckii* subsp. *bulgaricus* MSD231, and *Streptococcus thermophilus* AAE84, respectively. Every part was redivided into 6 groups, where the first and second groups were set as a negative control (without AgNPs) and positive control (formalin 0.4%), respectively. The 25, 50, 100, and 200 $\mu g\,mL^{-1}$ of AgNPs were individually added to the 3rd, 4th, 5th, and 6th groups. Every group was redivided into two subgroups, where the first and

second subgroups were incubated at 37°C and 43°C, respectively. The determination of milk acidification (pH, alcohol precipitation, and clot on boiling), proteolytic, and lipolytic activity was used as an evaluation tool of preservative efficacy of AgNPs in the composite milk samples.

2.12.2. Alcohol Precipitation Test. This test is carried out by mixing equal volumes of 68% of ethanol solution and milk in test tubes. If the acidity of the tested composite milk is normal (0.14 to 0.18%), there will be no clotting, coagulation, or precipitation. The presence of clots points out the acidity of the tested composite milk sample ranged from 0.21 to 0.23%.

2.12.3. Clot on Boiling (COB) Test. The COB is a very easy test used to evaluate the quality of milk. A defined volume of composite milk sample in the test tube is boiled. The sample cannot withstand boiling, and coagulation was created on the wall of the test tube due to high acidity of the sample (0.23 to 0.28%).

2.12.4. Proteolytic Activity. The proteolytic activity of milk samples was determined according to El Dessouky Abdel-Aziz et al. [25] with slight modification. Briefly, approximately 0.5 mL buffer (4.5 mM KH_2PO_4; pH 7.5) was transferred into a screw-capped test tube and was mixed with 24 mg of Azocoll, followed by incubation for 5 min at 36°C. Then, 0.5 mL of milk sample was added into the tube and mixed with a vortex mixer for 45 s followed by incubation for 30 min at 36°C. The screw-capped tubes were transferred to the icebox, for stopping the reaction. The filtration of the mixture was carried out by using Whatman No.4 filter papers. The absorption of released azo dye was determined by using a UV spectrophotometer at 520 nm. One unit of activity was defined as the amount of enzyme that will catalyze the release of sufficient azo dye to produce an absorbance change of 0.001 in 30 min at 520 nm. Results are expressed as the time required to increase one unit of activity compared with the initial point.

2.12.5. Lipolytic Activity of Composite Milk Sample. The lipolytic activity of the tested milk samples was determined by estimating the time required to liberate estimable free fatty acids (FFA) according to El Dessouky Abdel-Aziz et al. [25], with slight modification. Briefly, a volume of composite milk sample (5 mL) mixed with 25 mL ethanol was mixed with 10 mL, and then 3 drops of 1% phenolphthalein indicator solution were added. The titration of the mixture was performed by using potassium hydroxide (0.05 N). The titration of the mixture was at the endpoint when the pinkish color of the mixture appeared and persisted for 30 seconds. The calculation of % FFA depended on the following equation using the acid values and the value of the molar mass of oleic acid for the studied samples. Results are expressed as the time required to increase 1% of FFA compared with the initial point.

$$\text{Free fatty acid } [\%(\text{as oleic acid})] = \frac{T \times N \times 282 \times 100}{W \times 1000}, \quad (1)$$

where T is the volume of titrant, N is the normality of KOH, the molecular weight of oleic acid is 282, and W is the weight of the sample.

2.13. Infrared Analyzer for Composite Milk Analysis. The chemical composition analysis of the composite milk sample was carried out by MilkoScan (FOSS MilkoScan FT120) according to ISO [26].

2.14. Statistical Analysis. The data were analyzed with one-way ANOVA (analysis of variance) to determine the significant differences between the means by Tukey's HSD test at $P < 0.05$ using SAS (version 9.1, SAS Institute, NC, USA). The probit analysis was used to calculate the values of IC_{50} (concentrations of the silver nanoparticles that produce 50% inhibition on the cell lines viability) by SAS (version 9.1, SAS Institute, Cary, NC, USA).

3. Results and Discussion

3.1. Chemical Analysis of Crude Polysaccharides. The polysaccharide yield was 10.4% on the dry matter basis of the seeds used to prepare the extract (Table 1). However, the polysaccharide yield from *L. leucocephala* polysaccharide is 20% (*w*/*w*) [21]. The chemical composition of LLPs revealed the presence of total carbohydrate content (85.9%), total reducing sugars (10.4%), total polysaccharide (75.5%), crude protein (4.88%), and total ash (2.05%) (Table 1). Remarkably, LLPs contain a low level of total polyphenols as 35.3 mg GAE/g LLPs. The chemical analysis of LLPs in this study agreed to some extent with that obtained by the previous report [27]. In this work, *L. leucocephala* inactively extracted polysaccharide that contains total carbohydrates and total conjugated protein by 76.2 and 4.2%, respectively, with a trace content of total phenols by 38.32 mg GAE/g [27]. In another example, the total polyphenols in the crude polysaccharides were 21.6 and 16 mg GAE/g when the solid-liquid extraction method is used by methanol and ethanol, respectively [28, 29]. Additionally, the presence of low levels of proteins and ash in LLPs has been reported [21].

The TLC profile of LLPs presented two monosaccharides. These monosaccharides were assessed as mannose and galactose in comparison to Rf values of standard monosaccharides. Rf value was noted to be related to that detected with galactose and mannose, so it can be termed as galactomannan gum. Additionally, the NMR analysis was done to confirm the galactomannan structure of LLPs (Figure 1). ^{1}H NMR spectrum exposed two anomeric protons at δ = 4.70 ppm and δ = 4.89 ppm, assignable to H-1 of β-d-mannopyranosyl and α-d-galactopyranosyl residues, respectively (Figure 1). Moreover, the peaks between δ = 4.01 and 3.69 ppm corresponded to H_2 to H_6. These ^{1}H NMR chemical shifts were in line with the values obtained in the previous studies [21, 30, 31]. These findings have confirmed the galactomannan structure of the crude polysaccharide isolated from seeds of *L. leucocephala* with a linear chain of D-mannopyranosyl residue connected through β (1→4) linkage and α-d-galactopyranosyl residue at O-6 of mannose unit. Overall, extraction of water-soluble galactomannans

Table 1: Chemical composition of LLPs and monosaccharide profile.

Chemical composition of LLPs							
Yield (%)	Total sugars (%)	Reducing sugars (%)	Total polysaccharides (%)	Crude protein (%)	Moisture (%)	Ash (%)	Total polyphenols (mg GAE/g)
10.4%	85.9	10.4	75.5	4.88	3.95	2.05	35.3

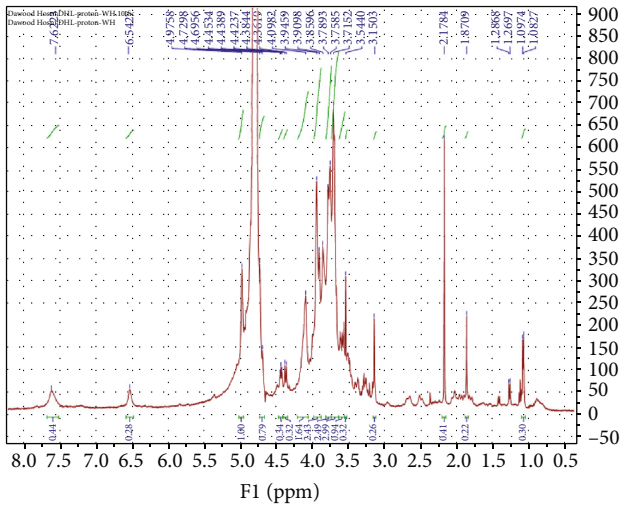

Figure 1: ^{1}H-NMR of the polysaccharides extracted from *Leucaena leucocephala* seeds.

from the seeds of *L. leucocephala* with different M/G molar ratios has been reported [30, 32]. In this context, the molecular weight of LLPs was evaluated by high-performance gel permeation chromatography. The peak of elution was nearly single, equivalent to the feature of homogeneous distribution. The molecular weight of LLPs was calculated to be 3.008×10^4 Da (Figure 2(a)). The molecular weight of LLPs in this study was lesser than that of galactomannan isolated from the same part of the plant as 6.4×10^4 Da [30] as well as galactomannans isolated from other plants [33, 34].

The Fourier-transform infrared spectroscopy (FTIR) is one of the most useful and commonly used analytical means for identifying the functional groups of different macromolecules. The FTIR spectra of LLPs displayed different absorption peaks at 3449, 2922, 1642, 1406, 1255,1226, 1150, 1074, 1024, 870, and 816 cm^{-1}, respectively (Figure 2(b)). The values listed below confirmed the galactomannan structure of LLPs, where the broad band at 3449 cm^{-1}, are qualified to hydroxyl groups (O-H) present in these materials. Peak stretching at 2922 cm^{-1} was associated with the stretching vibration of C-H. The peaks at 1255 and 1226 cm^{-1} are most possibly from the C-O group of polyols of glucans and flavones [35] The absorption peaks at 1150, 1074, and 1024 cm^{-1} presented the stretching vibration of C-OH from the mannose structures [36]. The bands at 870 and 816 cm^{-1} were allocated to the anomeric configuration of β-D-mannopyranosyl and α-D-galactopyranosyl units, respectively; similar observations have been reported [34, 37]. On the other hand, the sharp band at 1642 cm^{-1} represents the presence of the carbonyl group C=O of the –NH-C=O amide bond stretching. The relative absorption peak is at 1406 cm^{-1} for N-H and methylene bending vibration. Therefore, the peaks at 1642 and 1406 cm^{-1} might be related to the low content of protein in crude LLPs.

3.2. Characterization of the Silver Nanoparticles. Numerous methods have been adapted for the biosynthesis of AgNPs using plant extracts [38]. Biosynthesis of AgNPs using macroalgae extracted polysaccharides, as reductant for silver ions as well as stabilizing agents for the synthesized AgNPs, has been stated [39]. Likewise, in this work, a well-stabilized AgNP solution was prepared using the extracted polysaccharides from *L. leucocephala* seed wastes as reducing agents for silver ions to produce AgNPs. Practically, AgNPs show brownish color in an aqueous solution due to excitation of surface plasmon vibration of AgNPs [40]. Consequently, the reduction of Ag^+ to AgNPs through trials could be confirmed by a color change from pale yellow to dark brown which was noted systematically by the UV-Vis spectroscopy (Figure 3(a)).

3.2.1. UV-Vis Spectroscopy. The ultraviolet-visible spectroscopy is an initial step for analyzing the formation of silver nanoparticles in an aqueous solution. Therefore, the polysaccharides along with $AgNO_3$ were subjected to bioreduction reaction, and the change in color to yellowish brown, indicating the formation of AgNPs. The silver surface plasmon resonance was detected at 448 nm (Figure 3(b)). In a previous report, Gengan et al. [41] itemized that the maximum absorbance occurred at 448 nm due to the existence of AgNPs. The characteristic silver surface plasmon resonance bands were found around 400-450 nm [42]. The mechanism of silver ions reduction to nanoparticles using polysaccharides extracted from *L. leucocephala* seed wastes might be due to the existence of functional hydroxyl groups in both monosaccharide units and related phenolics responsible for the development of AgNPs. These results are in harmony with previous researchers [43, 44].

3.2.2. FTIR Analysis. FTIR spectroscopy could be efficiently exploited for understanding the degree and nature of the interaction between two or more chemical species during the formation of nanoparticles. The results showed that all identified peaks in LLPs were shifted to some extent in AgNP-LLPs affirming the production of polysaccharide-capped AgNPs (Figure 2(b)). The presence of a peak at 3422 cm^{-1} in AgNP-LLPs is assigned for hydroxyl stretching, offering the capping efficacy of LLPs. The shifted peak from 1406 to 1386 cm^{-1} in AgNP-LLPs indicated the probable role of the trace proteins in the formation of AgNPs. Remarkably, it is well known that proteins can bind to the AgNPs

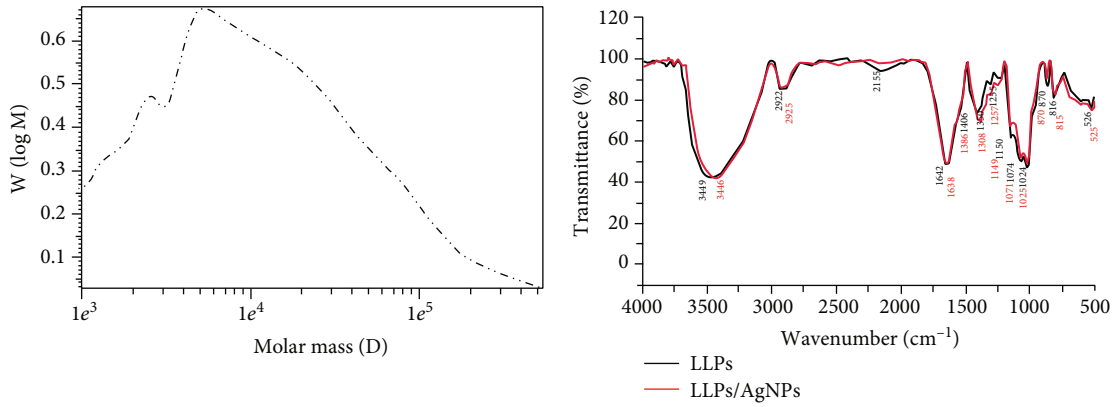

(a) (b)

Figure 2: Molecular weight of polysaccharides extracted from the seeds of *Leucaena leucocephala* (a). FTIR pattern of polysaccharides extracted from the seeds of *L. leucocephala* and their AgNPs (b).

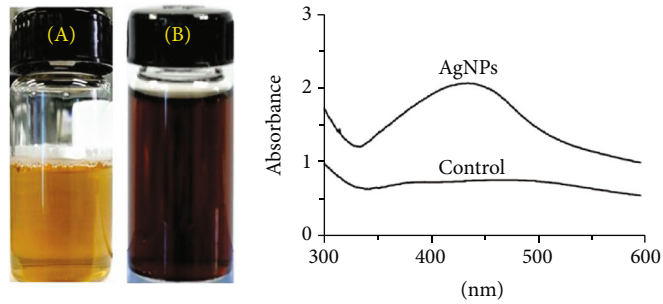

(a) (b)

Figure 3: (a) The reaction mixture color was changed from yellow (a) to reddish brown (b) after the addition of $AgNO_3$ solution (0.1 mM) to aqueous polysaccharides of *Leucaena leucocephala* seeds. (b) UV-Vis spectrum of AgNPs synthesized using polysaccharides extracted from *L. leucocephala* seeds.

via the free amine groups in their backbone structure [45]. The changes in FTIR spectrum in this study between 1255 and 1226 cm^{-1} might reflect the probable role of the C-O group of polyols such as hydroxyl flavones in the formation of AgNP-LLPs [35]. Overall, the results confirm the theory that the phenolic constituents and polypeptide structure are critical in the development and stabilization of different metal ion nanoparticles. These functional groups may shield the surface of silver ions as capping mediators that stabilize the nanoparticles, but the full mechanism assumed in the synthesis of AgNPs is still debated. Moreover, polyols like different polyphenols and polysaccharides that reduce silver ions may perform an identical role in the construction of AgNPs from *L. leucocephala* [46, 47].

3.2.3. X-Ray Diffraction (XRD). The crystallinity of formulated AgNP-LLPs was tested by XRD. Its pattern presented diffraction peaks at 38.27°, 46.27°, 64.63°, and 77.66° which can be indexed to the planes (111), (200), (220), and (311), respectively (Figure 4(a)). The identified crystalline peaks in the present work represented planes of a face-centered cubic lattice of silver; parallel observations have been documented in different studies [48–50]. Unknown crystalline peaks (27.89°, 32.30°, and 54.79°) are also evident in many reports in which the XRD pattern contains the relevant 2θ range [51]. These peaks are due to the organic molecules which occur in the extract.

3.2.4. Energy-Dispersive Spectroscopy (EDS). The EDS spectrum revealed a strong signal peak at ~3 keV, which confirms the occurrence of elemental silver in the produced nanosilver synthesized by polysaccharides (Figure 4(b)). In a similar study, Jagtap and Bapat [52] described the formation of irregular-shaped AgNPs at 2.98 keV using the seed extract of *Artocarpus heterophyllus*. The presence of a signal peak for carbon (C) in the EDS spectrum is possibly due to the structure of the polysaccharides present in the seeds of *L. leucocephala*, which is an added benefit in the green chemical synthesis. Our results strongly confirmed that the polysaccharides extracted from *L. leucocephala* seeds might act both as reducing and stabilizing agents in the production of AgNPs.

3.2.5. SEM and TEM Observations. Scanning electron microscopy (SEM) is a qualitative tool to examine the surface morphology of polysaccharides [53]. The surface of polysaccharides (LLPs) is relatively homogeneously smooth and consists mainly of randomly distributed particles under observations by SEM (Figure 5(a)). Meanwhile, the

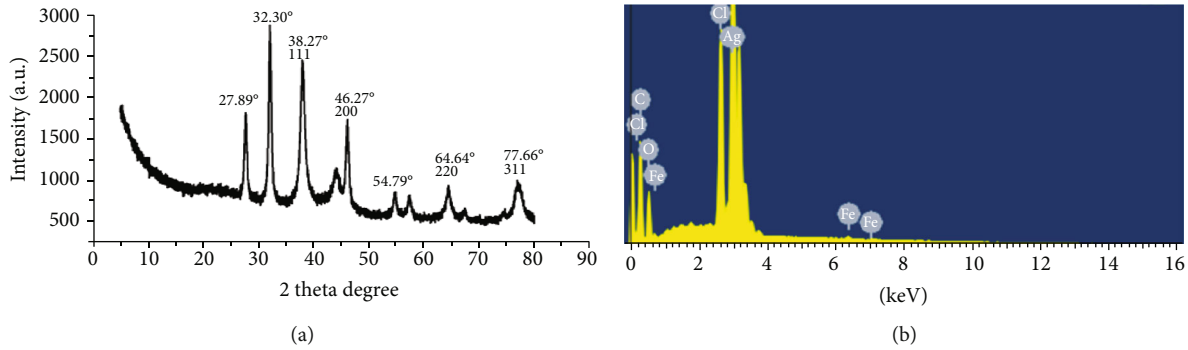

Figure 4: XRD spectrum of AgNPs synthesized by reducing 0.1 mM $AgNO_3$ using polysaccharides extracted from *Leucaena leucocephala* seeds (a). EDS pattern of the synthesized AgNPs from polysaccharides of *L. leucocephala* seeds (b).

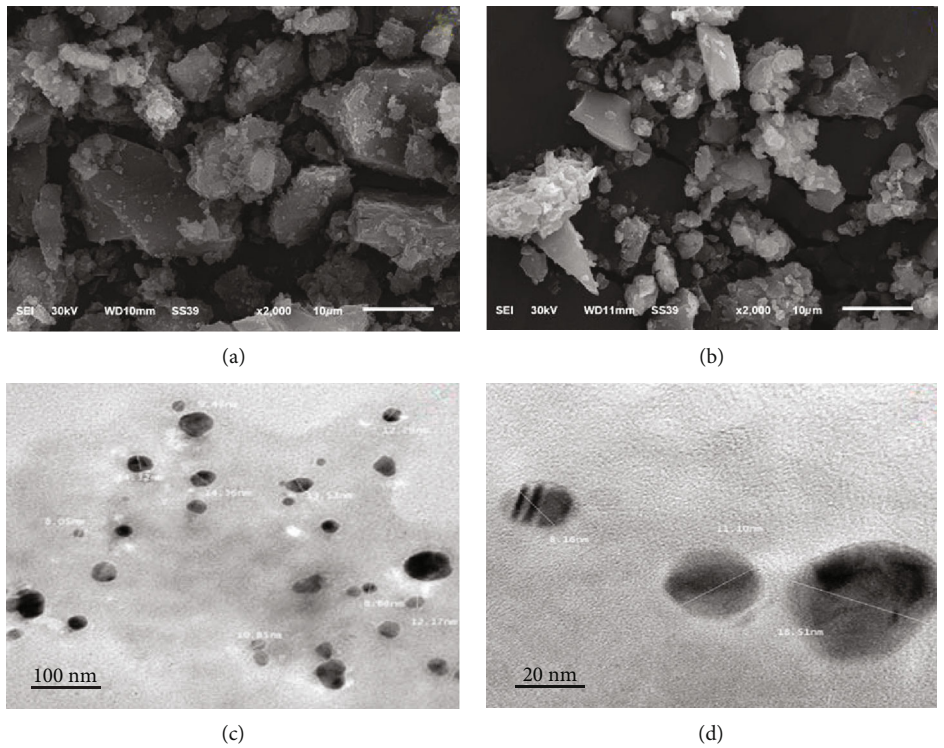

Figure 5: SEM micrograph of polysaccharides extracted from *Leucaena leucocephala* seeds (a). SEM micrograph of AgNPs synthesized by adding 0.1 mM $AgNO_3$ to polysaccharides of *Leucaena leucocephala* seeds (b). TEM images of biologically synthesized Ag nanoparticles using polysaccharides of *L. leucocephala* seeds (C&D).

morphological change after AgNP formation is not fully clear (Figure 5(b)). The SEM images of AgNP-impregnated LLPs were roughly spherical in shape and confirm the existence of silver in the polysaccharides. In other words, the silver nanoparticles from LLPs are monodisperse with a spherical shape and tribute among the polysaccharides. Similarly, the spherical shape of silver nanoparticles in polysaccharide-rich extracts has been reported [54, 55]. It has been exposed that the smaller size of AgNPs at pH 7 is more effective concerning its prospective applications [50]. So, the size, shape, and surface morphology of the produced AgNPs were characterized using transmission electron microscopy (TEM). The TEM images of AgNPs made by polysaccharides extracted from *L. leucocephala* seeds show that the particles are almost spherical with a size ranging from 8 to 20 nm (Figures 5(c) and 5(d)). These findings also confirm the monodisperse nature of AgNPs. Interestingly, the size range of AgNPs in this study was lower than those obtained using other polysaccharide-rich extracts [56, 57]. The size dissimilarity shown in Figure 5 may be due to the attendance of other organic ingredients in LLPs which are complicated in reducing and stabilizing AgNPs during their producing stage [58]. Overall, submicroparticles with a size below 1000 nm are adequate nanometric carriers used to deliver drugs or different types of biomolecules [59].

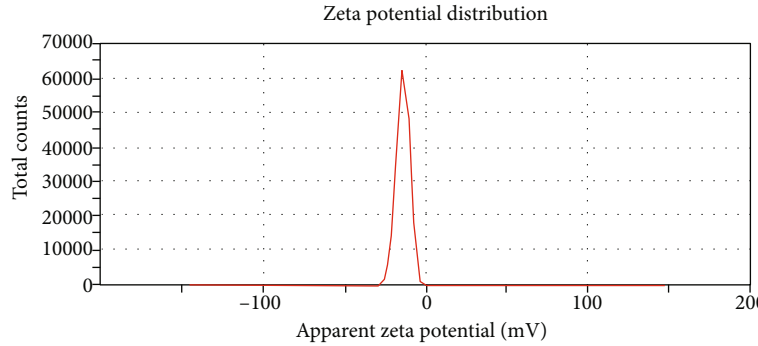

Result

		Mean (mV)	Area (%)	St dev (mV)
Zeta potential (mV): −14.2	Peak 1:	−14.2	100.0	4.14
Zeta deviation (mV): 4.14	Peak 2:	0.00	0.0	0.00
Conductivity (mS/cm): 0.342	Peak 3:	0.00	0.0	0.00
Result quality: Good				

Figure 6: Zeta potential measurement of AgNPs synthesized from polysaccharides of the seeds of *Leucaena leucocephala*.

Table 2: Antitumor activity of silver nanoparticles synthesized by polysaccharides extracted from *Leucaena leucocephala* seeds against breast cancer (MCF-7), liver carcinoma (HEPG-2), and colon carcinoma (HCT-116) cell lines at different concentrations.

Concentration (μg mL^{-1})	Cell inhibition (%)								
	MCF-7			HEPG-2			HCT-116		
	AgNPs	5-FU	LLPs	AgNPs	5-FU	LLPs	AgNPs	5-FU	LLPs
6.25	29.6 ± 0.4^{a}	27.4 ± 0.5^{b}	0 ± 0.0^{c}	34.1 ± 0.9^{a}	30.6 ± 0.7^{b}	3.3 ± 0.2^{c}	32.4 ± 0.8^{a}	26.2 ± 0.8^{b}	0 ± 0.0^{c}
12.5	42.9 ± 0.9^{b}	51.9 ± 0.3^{a}	0.3 ± 0.1^{c}	55.5 ± 0.9^{b}	60.5 ± 0.6^{a}	3.6 ± 0.2^{c}	57.1 ± 0.9^{b}	59.4 ± 0.6^{a}	1.2 ± 0.2^{c}
25	58.8 ± 1.4^{b}	70.6 ± 0.7^{a}	3.6 ± 0.7^{c}	71.8 ± 0.8^{b}	78.6 ± 0.6^{a}	15.2 ± 0.6^{c}	65.6 ± 0.3^{b}	73.9 ± 1.0^{a}	3.0 ± 0.4^{c}
50	77.3 ± 0.8^{b}	87.3 ± 0.8^{a}	7.6 ± 1.0^{c}	83.2 ± 0.7^{b}	90.7 ± 1.0^{a}	29.9 ± 1.2^{c}	78.7 ± 0.9^{b}	83.6 ± 1.2^{a}	6.5 ± 0.6^{c}
100	88.9 ± 0.5^{b}	96.6 ± 0.7^{a}	4.3 ± 0.5^{c}	90.1 ± 1.0^{a}	98.4 ± 0.6^{a}	53.6 ± 0.7^{c}	87.3 ± 1.1^{b}	91.9 ± 0.9^{a}	15.7 ± 0.7^{c}
IC_{50} (μg mL^{-1})	22.5	11.9	>100	12.3	10.8	90.7	8.9	7.3	>100

Silver nanoparticles (AgNPs), 5-fluorouracil (5-FU), and polysaccharides extracted from *Leucaena leucocephala* seeds (LLPs). Results represent means ± standard error (SE) for two experiments. Different letters in the same row are significantly different according to Tukey's HSD test at $P < 0.05$ for each cell line.

3.2.6. Zeta Potential Measurement. Aggregation of particles is a key aspect affecting the suspension stability of the debris particles in aqueous solutions. The aggregation or dispersion of colloidal particles is assessed by the balance between the Van der Waals force and electrical double-layer repulsive forces when particles closely approach one another [60]. The zeta potential is used to describe the surface charge and stability of nanoparticles in aqueous media. It is recorded at or near the border of the diffuse film on the surface of the particle; therefore, the stability of any suspension is closely related to the zeta potential of suspended particles [61]. Additionally, it is well known that a suspension with a zeta potential value closer to zero has no force to stop the aggregation of the particles. Contrarily, a suspension with a higher negative or positive zeta potential value has a higher tendency of its particles to repel with each other, and therefore, no accumulation of particles is expected. In neutral pH, the value of zeta potential for AgNPs in this study was found to be -14.2 mV with a single peak revealing the stability of the biosynthesized silver nanoparticles (Figure 6), and the related values have been described by Wang et al. [60] and Elamawi et al. [62]. In other words, the value of the zeta potential of AgNPs synthesized by polysaccharides extracted from *L. leucocephala* seeds reflects the presence of a notable electrostatic repulsion between particles which can block the aggregation and precipitation of debris particles of AgNPs. This was confirmed by our experimental test displaying the debris could not be aggregated by high-speed centrifugation at $8000 \times g$ for 45 min. Overall, the stability of nanoparticles in an aqueous solution is very essential regarding antimicrobial applications as unstable AgNPs will not be able to disperse homogeneously, hence decreasing the efficiency.

3.3. Antitumor Activity. In the recent decade, polysaccharide-based metal nanoparticles are delivering remarkable applications in nanomedicine, including avoidance, diagnosis, and

Table 3: Effect of silver nanoparticles synthesized by polysaccharides extracted from *Leucaena leucocephala* seeds on mycelial growth of fungal pathogens at different concentrations.

Fungi	Mycelial growth inhibition (%)			
	300 $\mu g\,mL^{-1}$	500 $\mu g\,mL^{-1}$	700 $\mu g\,mL^{-1}$	900 $\mu g\,mL^{-1}$
Alternaria alternata	0.0 ± 0.0^{d}	0.0 ± 0.0^{d}	15.6 ± 1.2^{gh}	25.6 ± 8.0^{g}
Aspergillus flavus	0.0 ± 0.0^{d}	2.9 ± 6.0^{d}	17.0 ± 1.2^{fgh}	42.2 ± 1.2^{f}
Aspergillus parasiticus	0.0 ± 0.0^{d}	0.0 ± 0.0^{d}	21.9 ± 0.8^{ef}	37.8 ± 0.5^{f}
Bipolaris hawaiiensis	28.5 ± 0.9^{a}	40.7 ± 1.2^{a}	52.6 ± 0.8^{b}	85.6 ± 0.6^{a}
Bipolaris spicifera	0.0 ± 0.0^{d}	0.0 ± 0.0^{d}	11.5 ± 0.9^{h}	28.5 ± 0.6^{g}
Botrytis cinerea	5.9 ± 0.9^{c}	19.3 ± 1.1^{b}	32.2 ± 1.2^{c}	68.1 ± 0.8^{cd}
Cochliobolus cynodontis	4.4 ± 0.6^{c}	16.3 ± 0.9^{b}	25.9 ± 1.2^{de}	71.5 ± 1.2^{c}
Fusarium oxysporum	0.0 ± 0.0^{d}	16.7 ± 1.2^{b}	28.5 ± 0.9^{cd}	52.9 ± 0.9^{e}
Fusarium sambucinum	0.0 ± 0.0^{d}	11.5 ± 0.9^{c}	20.4 ± 1.1^{efg}	63.7 ± 1.4^{d}
Penicillium digitatum	12.2 ± 1.1^{b}	40.7 ± 0.8^{a}	65.9 ± 1.4^{a}	78.5 ± 0.9^{b}

Results represent means ± standard error (SE) for two experiments. Different letters in the same column are significantly different according to Tukey's HSD test at $P < 0.05$.

treatment of different tumors. Its sophisticated targeting scheme and multifunctional characters have notable advantages in the enhancement of pharmacokinetics and pharmacodynamics profiles compared to traditional therapeutics [56]. Therefore, the application of different polysaccharide-based metal nanoparticles in cancer treatment has been developed as a promising area in nanotechnology [60].

In the current study, the antitumor property of the different AgNPs concentrations ranging between 6.25 and 100 $\mu g\,mL^{-1}$ was examined *in vitro* against liver carcinoma (HEPG-2), colon carcinoma (HCT-116), and breast cancer (MCF-7) cell lines and compared with 5-fluorouracil (5-FU). The silver nanoparticles obtained from *L. leucocephala* polysaccharides exhibited cytotoxic activity mostly equivalent to the positive control (5-FU) against all cancer cell lines in a concentration-related manner (Table 2). Our results displayed that HCT-116 cell proliferation was significantly inhibited by AgNPs with an IC_{50} value of 8.9 $\mu g\,mL^{-1}$. Besides, AgNPs exhibited considerable anticancer activity against HEPG-2 and MCF-7 cell lines with IC_{50} of 12.3 and 22.5 $\mu g\,mL^{-1}$, respectively. In this context, Tran et al. [57] recorded the slightly higher antitumor activity of chitosan with AgNPs against HEPG-2 and MCF-7 cell lines with IC_{50} values of 6.09 and 5.71 $\mu g\,mL^{-1}$, respectively. Likewise, chitosan and silver nanocomposite showed a great inhibition on lung cancer cells (A549) with a considerably low value of IC_{50} by 29.35 $\mu g\,mL^{-1}$ [63].

In general, AgNPs with a smaller size range showed higher biological activities [64]. Consequently, the discrepancy regarding cytotoxicity IC_{50} values of polysaccharide-based AgNPs is highly associated with their type, the size of examined cells, and the bioactive molecules tied to them since secondary metabolites may have antitumor efficacy. The mode of action of AgNPs against tumor cell lines is not entirely understood, but cell oxidative stress initiated by the propagation of ROS can be caused by the cellular uptake of AgNPs [64]. Apoptosis is reflected as one of the biotic actions that disrupt the abnormal cell and is a suitable sign for the investigation of cytotoxicity [65, 66].

The results of the current study presented that the galactomannan-rich polysaccharides recorded a relatively low value of IC_{50} against HEPG-2 cells compared with other cell lines, indicating its higher selectivity to liver cancer. This might be due to the presence of numerous side-chain galactose units that might easily bind with galactose-specific receptors of the cancer cell surface, modify the cancer surface physiology, and probably influence the distribution of bioactive ingredients and drugs to the cancer cells [67]. Moreover, galactomannan-rich polymers have different biological activities such as immunostimulation, anticancer, and cancer chemopreventive [9, 68, 69].

According to the results obtained, galactomannan-rich polysaccharides recorded the highest IC_{50} values, which reflected their weak antitumor activity against all cell lines. Therefore, the transformation of *L. leucocephala* galactomannan-rich polysaccharides into silver nanoparticles significantly increased their antitumor potential against all tested cell lines without any selectivity. In the same way, *L. leucocephala* galactomannan-sulfated derivatives recorded high cytotoxicity against HEPG-2, MCF-7, and 1301 cell lines [27].

3.4. Antifungal Activity. Metal nanoparticles display a great ratio of surface area-to-volume and show antimicrobial activity because of their ease of interaction with cellular membranes [70]. Many silver-containing compounds, particularly AgNPs, have been used as antimicrobial agents to inhibit or to kill the growth of the plant and human pathogens [71]. There is an information frame on the antimicrobial potential of AgNPs biosynthesized by different species of plants, but insufficient attention has been focused on their potential antifungal properties [71]. Therefore, this study

focused on evaluating the antifungal activity of AgNPs against different fungal strains.

The results of the current showed that the inhibitory effect of AgNPs on the mycelial growth of all tested fungi was positively correlated to the concentration of AgNPs used (Table 3). At the concentration of 900 $\mu g\,mL^{-1}$, in particular, AgNPs caused a significant reduction in the growth of *B. hawaiiensis*, *P. digitatum*, *C. cynodontis*, and *F. sambucinum* by 85.6, 78.5, 71.5, and 63.7%, respectively. Furthermore, the results pointed to the fungus *A. alternata* being the most tolerant fungi, while the fungus *B. hawaiiensis* being more sensitive to the concentrations of AgNPs.

As documented by Bahrami-Teimoori et al. [72], the maximum of the antifungal activity of the biosynthesized AgNPs using the plant extract of *A. retroflexus* against different plant pathogenic fungi was reached at lower concentration (400 μg mL^{-1}). This could be explained by the presence of bioactive metabolites owning to the antifungal activity in the plant extracts.

AgNPs synthesized and stabilized by polysaccharides have effective antimicrobial properties on both Gram-positive and Gram-negative bacteria as well as a considerable antifungal activity [73]. Gram-negative bacteria were more probably to be affected than other microbes due to their membrane structure characterized by the negatively charged cell wall, which made it easier to attach the released Ag^{+}, which resulted in cell death [74]. The silver ions rapidly bind with the thiol (-SH) group of the lipid bilayer or membrane-bound proteins causing ion leakage and cell rupture as a result of membrane destabilization [75].

In fungi, the changes related to silver nanoparticles intensely suppress the regulatory functions of cell membrane ergosterol, predominantly during the normal binding process, as well as disrupt the electron transport chain (ETC, respiratory chain) by forming insoluble constituents in the cell wall due to the inactivation of the sulfhydryl group [76]. However, the full mechanism complicated in the antifungal property of AgNPs is still not entirely understood. The propagation of ROS and other free radicals and modulation of microbial signal transduction pathways have been identified as the most well-known modes of antimicrobial property of AgNPs penetrated inside the microbial cell [77].

In this context, a few studies have been conducted to estimate the antifungal activities of green biosynthesized AgNPs. Silver nanoparticles from microbial filtrates or plant extracts showed strong antifungal activity against several phytopathogenic fungi, including *F. oxysporum* [78], *Macrophomina phaseolina*, *A. alternata*, *Rhizoctonia solani*, *Sclerotinia sclerotiorum*, *B. cinerea*, *Curvularia lunata* [79], *A. flavus*, and *A. fumigatus* [80]. Interestingly, the antifungal potency of transparent nanocomposites composed of the polysaccharide of pollutant and silver against *A. niger* has been also evaluated [81].

The strains of the genus *Cochliobolus* and its asexual state *Bipolaris* largely spread and are both saprophytic as well as pathogenic to more than 60 different hosts [82]. They are accountable for critical spoilage to grasses and some economically important crops worldwide, comprising root rot, leaf spots in wheat and southern leaf blight of maize, black kernels of rice, spot blotches in barley and wheat, and eyespots and brown stripes in sugarcane [82, 83]. Besides, *Bipolaris* species are probably able to infect humans, particularly the species of *B. spicifera* which causes fungal peritonitis, fungal sinusitis, disseminated infection, keratitis, and meningitis; meanwhile, phaeohyphomycosis can also occur by *B. hawaiiensis* [82]. Hitherto, the present study is the first work reporting the strong antifungal effect of green synthesized AgNPs against the fungi of *B. hawaiiensis* and *C. cynodontis*.

3.5. Correlation between the Log of Cell Numbers (CFU/mL) and Milk Acidification (pH). The bacterial growth curves of *Escherichia coli* MSD102, *Enterococcus faecalis* MSD23, *Lactobacillus delbrueckii* subsp. *bulgaricus* MSD231, and *Streptococcus thermophilus* AAE84 presented a typical bacterial growth curve. This matched with the pH curve taken from pH measurements during the time, pointing out that pH values act as a surrogate sign for bacterial activity (Figure 7). The correlation between log CFU/mL and pH values was carried out. The selected function appreciated the data with an R^2 = 99.5, 99.3, 99.6, and 99.6% for bacterial growth curves of *E. coli*, *En. faecalis*, *L. delbrueckii* subsp. *bulgaricus*, and *S. thermophilus*, respectively, and their course has corresponded to the growth curve of bacterial culture. Bacteria were grown in batch culture, where most waste is not eliminated and no nutrients are added, following a reproducible pattern of growth indicated as the growth curve. The initial phase is called the lag phase, where pH values did not change, and log CFU/mL was low. The exponential phase started, where the log CFU/mL of bacteria began to increase, which was associated with a decrease in pH values. The highest cell number was not yet until the examined pH of 4.6. However, this was not critical, since merely the starting of acidification was determined. Moreover, the decline phase did not play any role in this study and was ruled out.

3.6. Practical Parameters for the Assessment of AgNPs Preserved Composite Milk Samples. Milk acidification was regarded as a measure of microbial growth, and the starting of milk acidification coincides with the point at which the pH decreases by 0.1 unit relative to the initial pH. Moreover, the alcohol precipitation and clot on boiling (COB) tests are used on the composite milk sample to present whether it will coagulate on both tests. These tests are particularly significant for monitoring the development of acidity in the milk. The clot on boiling (COB) test is less sensitive than the alcohol test. It is dependent on the milk protein tendency to get unstable because of disturbance in the salt balance of milk. On the other hand, lipolytic (production of free fatty acids "FFA") and proteolytic activity by some microorganisms during storage of composite milk samples were used as an important indicator for the stability of milk samples. The proteolytic and lipolytic activity was regarded as an indicator of microbial activity and the beginning of proteolytic or lipolytic activity corresponded to the point which the activity of proteolytic or lipolytic increases by 1.0 unit or 1% (as FFA), respectively, relative to the initial point. The milk

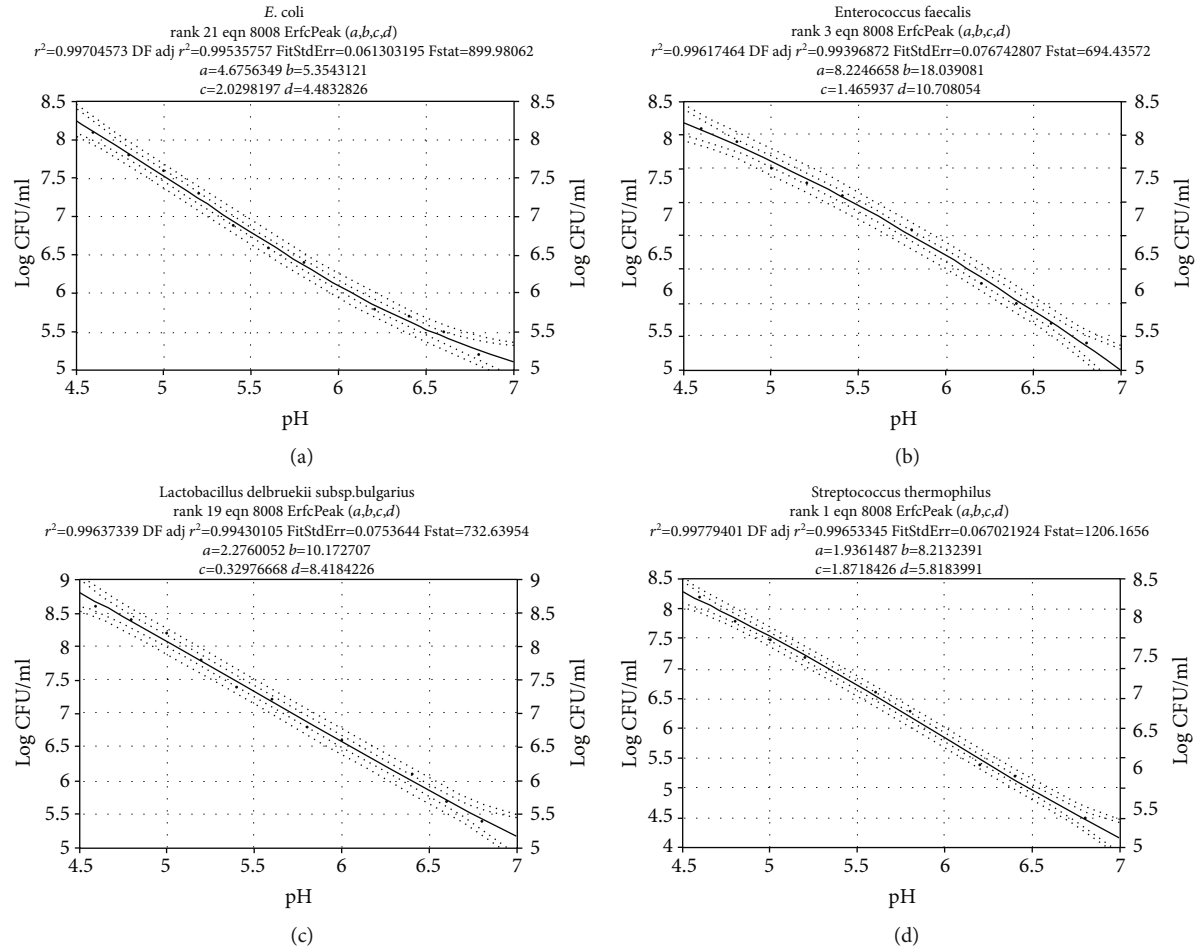

FIGURE 7: Correlation between the log of the average of cell count (CFU mL^{-1}) and milk acidification (pH) of (a) *E. coli* in milk at 37°C, (b) *En. faecalis* in whole milk at 37°C, (c) *Lactobacillus delbrueckii* subsp. *bulgaricus* in whole milk at 43°C, and (d) *Streptococcus thermophilus* in whole milk at 43°C. Starting of milk acidification was delineated as the point at which the pH value lowered by 0.1 units from the beginning value.

acidification (decline of pH, COB, and alcohol precipitation) and proteolytic and lipolytic activity by *E. coli*, *En. faecalis*, *L. delbrueckii* subsp. *bulgaricus*, and *S. thermophilus* could be slowed down by AgNP addition with different concentrations (Table 4). The concentration of AgNPs is directly proportional to the time required for alcohol precipitation, COB, a decline of pH value (0.1 unit relative to the initial pH), and lastly the increase of proteolytic and lipolytic activity (1.0 unit for the proteolytic activity or 1% FFA for lipolytic activity relative to the initial values) of tested composite milk samples.

No change occurred in all tested parameters until the end of this experiment (72 h), when using AgNPs at a concentration of 200 μg/mL and positive control with all tested bacterial strains. However, lower concentrations (25, 50, and 100 μg/mL) also exhibited a significant ($P < 0.05$) effect compared to the negative control (without chemical preservative) for all tested microorganisms (Table 4). The effect of temperature on different tested parameters depends on the bacterial strain, where the time required for all parameters at 43°C is less than incubated at 37°C, this is especially the case of composite milk samples which contain *S. thermophilus* or *L. delbrueckii* subsp. *bulgaricus*. On the contrary, the time needed for tested parameters at 43°C was more than the incubated composite milk samples containing *E. coli* or *En. faecalis* at 37°C (Table 4).

A concentration of 25 $\mu g\,mL^{-1}$ AgNPs is suitable for composite milk samples that were required short-term preservative, such as for obtaining the composite milk samples from the dairy farm to the laboratory for analysis; this concentration of AgNPs provided a small increase in shelf life but is not appropriate for composite milk samples held long-term. However, the addition of AgNPs (200 $\mu g\,mL^{-1}$) can extend the stability of the composite milk sample by ~3 days when compared with the other concentrations. Using 200 $\mu g\,mL^{-1}$ of AgNPs as a long-term preservative (longer than 3 days) will need further studies. The present study is consistent with Braun et al. [5], who found silver nanoparticles (100 $\mu g\,mL^{-1}$) to have antibacterial activity at different temperatures (23, 33, and 43°C). Previous measurements presented that extremely more silver nitrate has to be supplemented to milk for free Ag^+ to become available than in water, where milk components react with Ag^+; therefore, the practical use of nanosilver for the manufacture of dairy

Table 4: Milk acidification (pH, alcohol precipitation, and heat coagulation) and proteolytic and lipolytic activity changes by *E. coli*, *En. faecalis*, *L. delbrueckii* subsp. *Bulgaricus*, and *S. thermophilus* at 37 ± 1°C or 43 ± 1°C in the presence of 25, 50, 100, or 200 $\mu g\,mL^{-1}$ AgNPs compared with negative control (lacking AgNPs) or positive control (formalin 0.4%).

Treatments	Beginning acidification time (min)		Alcohol precipitation time (min)		Heat coagulation time (min)		Beginning proteolytic activity time (min)		Beginning lipolytic activity (FFA production time) (min)	
	37°C	43°C	37°C	43°C	37°C	43°C	37°C	43°C	37°C	43°C
Escherichia coli										
Negative control	95 ± 1.0^{d}	106.3 ± 0.6^{d}	212.67 ± 3.1^{d}	231.67 ± 1.2^{d}	248.67 ± 3.1^{d}	274 ± 1.5^{d}	142.7 ± 3.1^{d}	167.3 ± 1.5^{d}	161.3 ± 3.1^{d}	184.3 ± 3.1
Positive control	—	—	—	—	—	—	—	—	—	—
25 $\mu g\,mL^{-1}$	402 ± 2.0^{c}	421.7 ± 0.6^{c}	511.33 ± 3.1^{c}	528 ± 2.0^{c}	534 ± 3.0^{c}	554.33 ± 3.0^{c}	620.7 ± 2.5^{c}	643 ± 2.0^{c}	637.7 ± 3.5^{c}	672.3 ± 1.5
50 $\mu g\,mL^{-1}$	999.7 ± 1.5^{b}	1076.7 ± 2.1^{b}	1126.7 ± 2.5^{b}	1148.7 ± 1.5^{b}	1156.7 ± 2.5^{b}	1175.7 ± 2.5^{b}	1235 ± 3.6^{b}	1272.3 ± 4.0^{b}	1279.3 ± 2.5^{b}	1295.3 ± 4.0
100 $\mu g\,mL^{-1}$	1806.33 ± 0.6^{a}	1826.67 ± 1.5^{a}	1845 ± 2.0^{a}	1866 ± 2.0^{a}	1871.33 ± 3.1^{a}	1891.67 ± 2.5^{a}	1906.7 ± 2.5^{a}	1931.7 ± 3.1^{a}	1961 ± 3.6^{a}	1983 ± 1.0
200 $\mu g\,mL^{-1}$	—	—	—	—	—	—	—	—	—	—
Enterococcus faecalis										
Negative control	108 ± 1.0^{d}	116.7 ± 1.5^{d}	234.7 ± 2.1^{d}	244.3 ± 3.1^{d}	263.7 ± 3.5^{d}	293.3 ± 2.1^{d}	156.3 ± 2.5^{d}	174 ± 3.0^{d}	171.6 ± 2.5^{d}	195.3 ± 2.5^{d}
Positive control	—	—	—	—	—	—	—	—	—	—
25 $\mu g\,mL^{-1}$	388 ± 1.0^{c}	403.3 ± 0.6^{c}	485.7 ± 2.5^{c}	509.3 ± 2.5^{c}	514.3 ± 2.5^{c}	536.7 ± 2.5^{c}	592 ± 3.0^{c}	613.7 ± 4.0^{c}	616.6 ± 3.5^{c}	642.3 ± 4.5^{c}
50 $\mu g\,mL^{-1}$	912.3 ± 0.6^{b}	934.7 ± 1.5^{b}	987.7 ± 3.1^{b}	1009.3 ± 3.5^{b}	1031.3 ± 3.1^{b}	1049 ± 2.6^{b}	1079.3 ± 2.5^{b}	1119.6 ± 3.0^{b}	1157 ± 3.0^{b}	1194.3 ± 3.5^{b}
100 $\mu g\,mL^{-1}$	1672.67 ± 1.5^{a}	1687 ± 2.7^{a}	1721 ± 3^{a}	1737.7 ± 2.5^{a}	1754.6 ± 2.5^{a}	1779.7 ± 2.5^{a}	1794.3 ± 3.5^{a}	1807 ± 3.0^{a}	1820.7 ± 2.5^{a}	1837 ± 3.0^{a}
200 $\mu g\,mL^{-1}$	—	—	—	—	—	—	—	—	—	—
Lactobacillus delbrueckii subsp. *Bulgaricus*										
Negative control	112.5 ± 0.5^{d}	95.5 ± 0.5^{d}	234.7 ± 4.0^{d}	219 ± 1.5^{d}	287.7 ± 3.5^{d}	257 ± 4.0^{d}	171 ± 3.0^{d}	152.7 ± 4.0^{d}	179 ± 3.0^{d}	154.7 ± 0.5^{d}
Positive control	—	—	—	—	—	—	—	—	—	—
25 $\mu g\,mL^{-1}$	438.3 ± 2.5^{c}	409.3 ± 1.5^{c}	528.6 ± 2.5^{c}	494.7 ± 3.5^{c}	547.3 ± 4.5^{c}	506.3 ± 4.0^{c}	611.7 ± 3.5^{c}	586.3 ± 4.0^{c}	648.6 ± 4.0^{c}	614.7 ± 3.5^{c}
50 $\mu g\,mL^{-1}$	1201.33 ± 1.5^{b}	1176 ± 1.0^{b}	1283.6 ± 3.5^{b}	1241.3 ± 4.2^{b}	1318 ± 3.5^{b}	1305.6 ± 3.5^{b}	1345 ± 3.6^{b}	1328.3 ± 3.5^{b}	1370.6 ± 3.5^{b}	1344 ± 4.0^{b}
100 $\mu g\,mL^{-1}$	2003.67 ± 2.5^{a}	1994.7 ± 2.1^{a}	2157.6 ± 2.5^{a}	2124.3 ± 3.5^{a}	2191.7 ± 5.5^{a}	2154.6 ± 3.0^{a}	2234.7 ± 3.5^{a}	2215 ± 3.0^{a}	2271 ± 3.6^{a}	2253 ± 4.0^{a}
200 $\mu g\,mL^{-1}$	—	—	—	—	—	—	—	—	—	—
Streptococcus thermophilus										
Negative control	117.2 ± 0.3^{d}	96.3 ± 0.6^{d}	225 ± 1.5^{d}	200.3 ± 3.5^{d}	278 ± 3.0^{d}	245.3 ± 4.0^{d}	178.6 ± 3.0^{d}	157 ± 2.6^{d}	187.7 ± 3.0^{d}	162 ± 2.0^{d}
Positive control	—	—	—	—	—	—	—	—	—	—
25 $\mu g\,mL^{-1}$	532.7 ± 2.1^{c}	504.7 ± 0.6^{c}	623.6 ± 3.0^{c}	591.6 ± 3.2^{c}	643 ± 3.6^{c}	$6.9.7 \pm 2.5^{c}$	713 ± 3.0^{c}	694.6 ± 2.5^{c}	745.3 ± 3.0^{c}	736 ± 3.5^{c}
50 $\mu g\,mL^{-1}$	1303 ± 2.0^{b}	1285 ± 1.0^{b}	1384.3 ± 3.5^{b}	1354.6 ± 3.5^{b}	1412 ± 4.5^{b}	1389.7 ± 3.0^{b}	1435 ± 3.0^{b}	1424.6 ± 3.5^{b}	1454 ± 3.0^{b}	1433.7 ± 4.0^{b}
100 $\mu g\,mL^{-1}$	2085.67 ± 2.5^{a}	2038 ± 2.0^{a}	2236.7 ± 3.0^{a}	2223.7 ± 4.5^{a}	2294 ± 3.0^{a}	2276.3 ± 3.5^{a}	2341 ± 2.4^{a}	2317.3 ± 4.7^{a}	2371.7 ± 3.5^{a}	2337.3 ± 4.0^{a}
200 $\mu g\,mL^{-1}$	—	—	—	—	—	—	—	—	—	—

Note ($n = 3$; average ± standard diffusion): values in rows with different superscripts (a–d) have significant differences according to Tukey's HSD test at $P < 0.05$. – indicates that there is no change in tested parameters until 72 h.

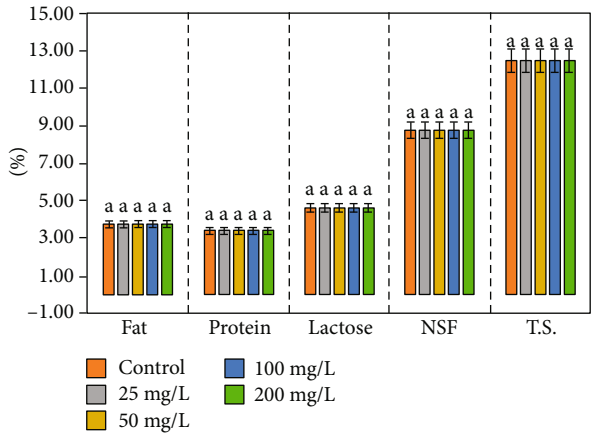

FIGURE 8: Average fat, protein, lactose, SNF, and TS readings for AgNPs (25, 50, 100, and 200 $\mu g\,mL^{-1}$) for the preserved and unpreserved portion of the same milk.

products is improbable, due to the required high concentrations of silver [5]. Heretofore, our study is the first work presenting the ability to use green synthesized AgNPs as a chemical preservative for composite milk samples.

3.7. The Influence of AgNPs with Different Concentrations on the Accuracy of Midinfrared Milk Component Testing. The essential part of our experiment was focused on studying the influence of AgNPs with different concentrations as chemical composite milk sample preservatives on the accuracy of milk-IR-analyses. The average values of the chemical composition parameters (fat, protein, lactose, solid not fat "SNF," and total solid "TS") of unpreserved milk and preserved milk stored at 4°C for 24 h are presented in Figure 8.

According to the ANOVA, there were no statistically significant differences ($P < 0.05$) in the average values of chemical parameters among the concentrations of AgNPs with analytes. A high concentration of AgNPs was used as a chemical preservative for milk samples compared with other preservatives, it did not affect the accuracy of milk-IR-analyses. However, the smallest influence of potassium dichromate on the milk-IR-analyses was achieved with 0.01% of potassium dichromate according to Kaylegian et al. [84]. Zajác et al. [85] also found that using extremely high concentrations (0.1 to 1%) of potassium dichromate, azidiol, bronopol, and microtabs leads to a statistically significant increase in the deviation between laboratory results. Up to the present, the current study is the first work to prove that the use of AgNPs with different concentrations as a chemical preservative for composite milk samples does not affect the accuracy of milk-IR-analyses compared with other chemical preservatives.

4. Conclusion

Silver nanoparticles (AgNPs) were synthesized using polysaccharides extracted from *Leucaena leucocephala* seeds as a bioreduction and capping agent. The biosynthesized AgNPs were confirmed by the UV-Vis spectroscopy at 448 nm. The XRD pattern showed four major peaks of the crystalline AgNPs. The presence of silver was confirmed by the ED spectrum. The SEM and TEM images revealed that the morphology of AgNPs was a spherical shape with no particle agglomeration, and the size ranged between 8 and 20 nm. The negative zeta potential by 14.2 mV indicated the enhanced stability of the silver nanoparticles. The biosynthesized AgNPs showed strong antitumor activity against the cell lines of colon carcinoma, liver carcinoma, and breast cancer in a concentration-dependent manner as well as remarkable antifungal effects on the growth of the plant and human fungal pathogens. The high concentration of AgNPs (200 $\mu g\,mL^{-1}$) provides a longer shelf life of composite milk samples compared with other concentrations of AgNPs. Besides, all concentrations of AgNPs had no influence on an accurate result of a composite milk sample analysis. This study presents an opportunity to obtain bioactive silver nanoparticles processing strong antitumor and antifungal activities from a cheap waste, i.e., seed crude polysaccharides. Additionally, this is the first work demonstrating the strong antifungal effect of green synthesized AgNPs against the fungi *B. hawaiiensis* and *C. cynodontis* which were critical pests for economically important crops. Also, our study is the first work offering the ability to use green synthesized AgNPs as the chemical composite of milk sample preservation.

Data Availability

All data generated or analyzed during this study are available from the corresponding author on reasonable request.

Conflicts of Interest

The authors declare no conflict of interest.

Authors' Contributions

Mohamed A. Taher is responsible for conceptualization, investigation, formal analysis, data curation, visualization, and writing—review and editing. Ebtihal Khojah is responsible for data curation, visualization, writing—review and editing—and funding acquisition. Mohamed Samir Darwish is responsible for conceptualization, investigation, formal analysis, data curation, visualization, and writing—review and editing. Elsherbiny A. Elsherbiny is responsible for investigation, data curation, and writing—review and editing. Asmaa A. Elawady is responsible for conceptualization, investigation, formal analysis, data curation, and visualization. Dawood H. Dawood is responsible for investigation, formal analysis, data curation, and validation. Mohamed A. Taher and Ebtihal Khojah contributed equally to this work.

Acknowledgments

We acknowledge the financial support from the Taif University Researchers (supporting project number TURSP-2020/307), 438 Taif University, Taif, Saudi Arabia.

References

[1] F. Rodríguez-Félix, A. G. López-Cota, M. J. Moreno-Vásquez et al., "Sustainable-green synthesis of silver nanoparticles using safflower (_Carthamus tinctorius_ L.) waste extract and its antibacterial activity," *J Heliyon*, vol. 7, no. 4, article e06923, 2021.

[2] A. Banerjee, U. Halder, and R. Bandopadhyay, "Preparations and applications of polysaccharide based green synthesized metal nanoparticles: a state-of-the-art," *Journal of Cluster Science*, vol. 28, no. 4, pp. 1803–1813, 2017.

[3] O. Gherasim, R. A. Puiu, A. C. Bîrcă, A.-C. Burduşel, and A. M. Grumezescu, "An updated review on silver nanoparticles in biomedicine," *Journal of Nanomaterials*, vol. 10, no. 11, 2020.

[4] D. C. Lekha, R. Shanmugam, K. Madhuri et al., "Review on silver nanoparticle synthesis method, antibacterial activity, drug delivery vehicles, and toxicity pathways: recent advances and future aspects," *Journal of Nanomaterials*, vol. 2021, 11 pages, 2021.

[5] S. Braun, V. Ilberg, U. Blum, and H. C. Langowski, "Nanosilver in dairy applications–antimicrobial effects on Streptococcus thermophilus and chemical interactions," *International Journal of Dairy Technology*, vol. 73, pp. 376–383, 2020.

[6] C. L. Del-Toro-Sánchez, F. Rodríguez-Félix, F. J. Cinco-Moroyoqui et al., "Recovery of phytochemical from three safflower (Carthamus tinctorius L.) by-products: antioxidant properties, protective effect of human erythrocytes and profile by UPLC-DAD-MS," *Journal of Food Processing and Preservation*, vol. 45, article e15765, 2021.

[7] V. C. Pandey and A. Kumar, "Leucaena leucocephala: an underutilized plant for pulp and paper production," *Genetic Resources and Crop Evolution*, vol. 60, no. 3, pp. 1165–1171, 2013.

[8] P. K. Jaiwal and R. P. Singh, "Applied genetics of leguminosae biotechnology," *Springer Science & Business Media*, vol. 10, 2013.

[9] H. Ramesh, K. Yamaki, and T. Tsushida, "Effect of fenugreek (Trigonella foenum-graecum L.) galactomannan fractions on phagocytosis in rat macrophages and on proliferation and IgM secretion in HB4C5 cells," *Carbohydrate Polymers*, vol. 50, pp. 79–83, 2002.

[10] R. Sumarny and P. Simanjuntak, *Antidiabetic activity of active fractions of Leucaena leucocephala (lmk)*, Dewit seeds in experiment model, 2010.

[11] A. Chowdhury, R. Banerji, G. Misra, and S. Nigam, "Studies on leguminous seeds," *Journal of the American Oil Chemists Society*, vol. 61, no. 6, pp. 1023-1024, 1984.

[12] A. Yepes and M. S. Buckeridge, "Respuestas de las plantas ante los factores ambientales del cambio climático global: Revisión," *Colombia forestal*, vol. 14, no. 2, pp. 213–232, 2012.

[13] A. Savale, S. Ghotekar, S. Pansambal, and O. Pardeshi, "Green synthesis of fluorescent CdO nanoparticles using Leucaena leucocephala L. extract and their biological activities," *Journal of Bacteriology & Mycology.*, vol. 5, p. 00148, 2017.

[14] Y. B. Aher, G. H. Jain, G. E. Patil et al., "Biosynthesis of copper oxide nanoparticles using leaves extract of Leucaena leucocephala L. and their promising upshot against diverse pathogens," *International Journal of Molecular and Clinical Microbiology*, vol. 7, pp. 776–786, 2017.

[15] S. Ghotekar, A. Savale, and S. Pansambal, "Phytofabrication of fluorescent silver nanoparticles from Leucaena leucocephala L. leaves and their biological activities," *Journal of Water and Environmental Nanotechnology*, vol. 3, pp. 95–105, 2018.

[16] D. H. Dawood, M. S. Darwish, A. A. El-Awady, A. H. Mohamed, A. A. Zaki, and M. A. Taher, "Chemical characterization of Cassia fistula polysaccharide (CFP) and its potential application as a prebiotic in synbiotic preparation," *RSC Advances*, vol. 11, no. 22, pp. 13329–13340, 2021.

[17] T. Masuko, A. Minami, N. Iwasaki, T. Majima, S.-I. Nishimura, and Y. C. Lee, "Carbohydrate analysis by a phenol-sulfuric acid method in microplate format," *Analytical Biochemistry*, vol. 339, no. 1, pp. 69–72, 2005.

[18] G. L. Miller, "Use of dinitrosalicylic acid reagent for determination of reducing sugar," *Analytical Chemistry*, vol. 31, no. 3, pp. 426–428, 1959.

[19] D. Pearson, *The Chemical Analysis of Foods*, Churchill Livingstone, Edinburgh London and New York, 7th ed. edition, 1976.

[20] M. A. Taher, E. Mennat Allah, L. K. Tadros, and M. I. Sanad, "The effects of new formulations based on gum Arabic on antioxidant capacity of tomato (Solanum lycopersicum L.) fruit during storage," *Journal of Food Measurement and Characterization*, vol. 14, no. 5, pp. 2489–2502, 2020.

[21] N. Mittal, P. Mattu, and G. Kaur, "Extraction and derivatization of Leucaena leucocephala (Lam.) galactomannan: optimization and characterization," *International Journal of Biological Macromolecules*, vol. 92, pp. 831–841, 2016.

[22] M. A. Garza-Navarro, J. A. Aguirre-Rosales, E. E. Llanas-Vázquez, I. E. Moreno-Cortez, A. Torres-Castro, and V. González-González, "Totally ecofriendly synthesis of silver nanoparticles from aqueous dissolutions of polysaccharides," *International journal of polymer science*, vol. 2013, 8 pages, 2013.

[23] V. Vichai and K. Kirtikara, "Sulforhodamine B colorimetric assay for cytotoxicity screening," *Nature Protocols*, vol. 1, no. 3, pp. 1112–1116, 2006.

[24] E. A. Elsherbiny, A. Y. El Khateeb, and N. A. Azzaz, "Chemical composition and fungicidal effects of Ocimum basilicum essential oil on Bipolaris and Cochliobolus species," *Journal of Agricultural Science and Technology*, vol. 18, pp. 1143–1152, 2016.

[25] M. El Dessouky Abdel-Aziz, M. Samir Darwish, A. H. Mohamed, A. Y. El-Khateeb, and S. E. Hamed, "Potential activity of aqueous fig leaves extract, olive leaves extract and their mixture as natural preservatives to extend the shelf life of pasteurized buffalo milk," *Food*, vol. 9, p. 615, 2020.

[26] ISO, E 4833-1, *Microbiology of the Food Chain-Horizontal Method for the Enumeration of Microorganisms-Part 1: Colony Count at 30 Degrees C by the Pour Plate Technique*, International Organization for Standardization, Geneva, Switzerland, 2013.

[27] A. M. Gamal-Eldeen, H. Amer, W. A. Helmy, R. M. Talaat, and H. Ragab, "Chemically-modified polysaccharide extract derived from Leucaena leucocephala alters Raw 264.7 murine macrophage functions," *International Immunopharmacology*, vol. 7, pp. 871–878, 2007.

[28] S. I. Mussatto, L. F. Ballesteros, S. Martins, and J. A. Teixeira, "Extraction of antioxidant phenolic compounds from spent coffee grounds," *Separation and Purification Technology*, vol. 83, pp. 173–179, 2011.

[29] A. Zuorro and R. Lavecchia, "Spent coffee grounds as a valuable source of phenolic compounds and bioenergy," *Journal of Cleaner Production*, vol. 34, pp. 49–56, 2012.

[30] N. Rahim, D. Kamarun, and M. R. Ahmad, "Isolation and characterization of galactomannan from seed of Leucaena

leucocephala," *Polymer Bulletin*, vol. 75, no. 5, pp. 2027–2037, 2018.

[31] H. A. Pawar and K. Lalitha, "Isolation, purification and characterization of galactomannans as an excipient from _Senna tora_ seeds," *International Journal of Biological Macromolecules*, vol. 65, pp. 167–175, 2014.

[32] A. L. R. Mercê, E. Fernandes, A. S. Mangrich, and M. R. Sierakowski, "Evaluation of the complexes of galactomannan of Leucaena leucocephala and Co2+, Mn2+, Ni2+ and Zn2+," *Journal of the Brazilian Chemical Society*, vol. 11, no. 3, pp. 224–231, 2000.

[33] J. X. Jiang, H. L. Jian, C. Cristhian, W. M. Zhang, and R. C. Sun, "Structural and thermal characterization of galactomannans from genus Gleditsia seeds as potential food gum substitutes," *Journal of the Science of Food and Agriculture*, vol. 91, no. 4, pp. 732–737, 2011.

[34] Y. Liu, W. Xu, F. Lei, P. Li, and J. Jiang, "Comparison and characterization of galactomannan at different developmental stages of Gleditsia sinensis Lam," *Carbohydrate Polymers*, vol. 223, article 115127, 2019.

[35] N. A. Begum, S. Mondal, S. Basu, R. A. Laskar, and D. Mandal, "Biogenic synthesis of au and ag nanoparticles using aqueous solutions of black tea leaf extracts," *Colloids and Surfaces B: Biointerfaces*, vol. 71, no. 1, pp. 113–118, 2009.

[36] G. Rajput, I. Pandey, and G. Joshi, "Carboxymethylation of Cassia angustifolia seed gum: synthesis and rheological study," *Carbohydrate Polymers*, vol. 117, pp. 494–500, 2015.

[37] H. N. Lavudi, S. Kottapalli, and F. M. Goycoolea, "Extraction and physicochemical characterization of galactomannans from Dichrostachys cinerea seeds," *Food Hydrocolloids*, vol. 82, pp. 451–456, 2018.

[38] G. Rajakumar and A. A. Rahuman, "Larvicidal activity of synthesized silver nanoparticles using _Eclipta prostrata_ leaf extract against filariasis and malaria vectors," *Acta Tropica*, vol. 118, no. 3, pp. 196–203, 2011.

[39] H. El-Rafie, M. El-Rafie, and M. Zahran, "Green synthesis of silver nanoparticles using polysaccharides extracted from marine macro algae," *Carbohydrate Polymers*, vol. 96, no. 2, pp. 403–410, 2013.

[40] P. Mulvaney, "Surface plasmon spectroscopy of nanosized metal particles," *Langmuir*, vol. 12, no. 3, pp. 788–800, 1996.

[41] R. Gengan, K. Anand, A. Phulukdaree, and A. Chuturgoon, "A549 lung cell line activity of biosynthesized silver nanoparticles using Albizia adianthifolia leaf," *Colloids and Surfaces B: Biointerfaces*, vol. 105, pp. 87–91, 2013.

[42] E. C. Njagi, H. Huang, L. Stafford et al., "Biosynthesis of iron and silver nanoparticles at room temperature using aqueous sorghum bran extracts," *Langmuir*, vol. 27, no. 1, pp. 264–271, 2011.

[43] J. Huang, Q. Li, D. Sun et al., "Biosynthesis of silver and gold nanoparticles by novel sundriedCinnamomum camphoraleaf," *Nanotechnology*, vol. 18, no. 10, article 105104, 2007.

[44] J. Kesharwani, K. Y. Yoon, J. Hwang, and M. Rai, "Phytofabrication of silver nanoparticles by leaf extract of Datura metel: hypothetical mechanism involved in synthesis," *Journal of Bionanoscience*, vol. 3, pp. 39–44, 2009.

[45] A. Gole, C. Dash, V. Ramakrishnan et al., "Pepsin– gold colloid conjugates: preparation, characterization, and enzymatic activity," *Langmuir*, vol. 17, no. 5, pp. 1674–1679, 2001.

[46] S. Azizi, M. B. Ahmad, F. Namvar, and R. Mohamad, "Green biosynthesis and characterization of zinc oxide nanoparticles using brown marine macroalga Sargassum muticum aqueous extract," *Materials Letters*, vol. 116, pp. 275–277, 2014.

[47] D. Mubarak Ali, N. Thajuddin, K. Jeganathan, and M. Gunasekaran, "Plant extract mediated synthesis of silver and gold nanoparticles and its antibacterial activity against clinically isolated pathogens," *Colloids and Surfaces B: Biointerfaces*, vol. 85, no. 2, pp. 360–365, 2011.

[48] M. Oves, M. Aslam, M. A. Rauf et al., "Antimicrobial and anticancer activities of silver nanoparticles synthesized from the root hair extract of _Phoenix dactylifera_," *Materials Science and Engineering: C*, vol. 89, pp. 429–443, 2018.

[49] D. Sheny, J. Mathew, and D. Philip, "Phytosynthesis of Au, Ag and Au–Ag bimetallic nanoparticles using aqueous extract and dried leaf of Anacardium occidentale," *Spectrochimica Acta Part A: Molecular and Biomolecular Spectroscopy*, vol. 79, pp. 254–262, 2011.

[50] A. Rafiq, K. Zahid, A. Qadir, M. N. Khan, Z. M. Khalid, and N. Ali, "Inhibition of microbial growth by silver nanoparticles synthesized from Fraxinus xanthoxyloides leaf extract," *Journal of Applied Microbiology*, vol. 131, no. 1, pp. 124–134, 2021.

[51] R. Kumar, S. M. Roopan, A. Prabhakarn, V. G. Khanna, and S. Chakroborty, "Agricultural waste Annona squamosa peel extract: biosynthesis of silver nanoparticles," *Spectrochimica Acta Part A: Molecular and Biomolecular Spectroscopy*, vol. 90, pp. 173–176, 2012.

[52] U. B. Jagtap and V. A. Bapat, "Green synthesis of silver nanoparticles using Artocarpus heterophyllus Lam. seed extract and its antibacterial activity," *Industrial Crops and Products*, vol. 46, pp. 132–137, 2013.

[53] Y.-J. Liu, X.-L. Mo, X.-Z. Tang et al., "Extraction optimization, characterization, and bioactivities of polysaccharides from Pinelliae Rhizoma Praeparatum Cum Alumine employing ultrasound-assisted extraction," *Molecules*, vol. 22, p. 965, 2017.

[54] R. D. Vasquez, J. G. Apostol, J. D. de Leon et al., "Polysaccharide-mediated green synthesis of silver nanoparticles from Sargassum siliquosum J.G. Agardh: assessment of toxicity and hepatoprotective activity," *OpenNano*, vol. 1, pp. 16–24, 2016.

[55] M. E. I. Badawy, T. M. R. Lotfy, and S. M. S. Shawir, "Preparation and antibacterial activity of chitosan-silver nanoparticles for application in preservation of minced meat," *Bulletin of the National Research Centre*, vol. 43, no. 1, p. 83, 2019.

[56] A. Wicki, D. Witzigmann, V. Balasubramanian, and J. Huwyler, "Nanomedicine in cancer therapy: challenges, opportunities, and clinical applications," *Journal of Controlled Release*, vol. 200, pp. 138–157, 2015.

[57] H. V. Tran, L. Dai Tran, C. T. Ba et al., "Synthesis, characterization, antibacterial and antiproliferative activities of monodisperse chitosan- based silver nanoparticles," *Colloids and Surfaces A: Physicochemical and Engineering Aspects*, vol. 360, no. 1-3, pp. 32–40, 2010.

[58] A. K. Mittal, Y. Chisti, and U. C. Banerjee, "Synthesis of metallic nanoparticles using plant extracts," *Biotechnology Advances*, vol. 31, no. 2, pp. 346–356, 2013.

[59] Z. Liu, Y. Jiao, Y. Wang, C. Zhou, and Z. Zhang, "Polysaccharides-based nanoparticles as drug delivery systems," *Advanced Drug Delivery Reviews*, vol. 60, no. 15, pp. 1650–1662, 2008.

[60] F. Wang, Y. Ma, Y. Liu et al., "A simple strategy for the separation and purification of water-soluble polysaccharides from the fresh Spirulina platensis," *Separation Science and Technology*, vol. 52, pp. 456–466, 2017.

[61] N. H. Tkachenko, Z. M. Yaremko, C. Bellmann, and M. M. Soltys, "The influence of ionic and nonionic surfactants on aggregative stability and electrical surface properties of aqueous suspensions of titanium dioxide," *Journal of Colloid and Interface Science*, vol. 299, no. 2, pp. 686–695, 2006.

[62] R. M. Elamawi, R. E. Al-Harbi, and A. A. Hendi, "Biosynthesis and characterization of silver nanoparticles using Trichoderma longibrachiatum and their effect on phytopathogenic fungi," *Egyptian Journal of Biological Pest Control*, vol. 28, no. 1, p. 28, 2018.

[63] N. Arjunan, H. L. J. Kumari, C. M. Singaravelu, R. Kandasamy, and J. Kandasamy, "Physicochemical investigations of biogenic chitosan-silver nanocomposite as antimicrobial and anticancer agent," *International Journal of Biological Macromolecules*, vol. 92, pp. 77–87, 2016.

[64] M. A. Raza, Z. Kanwal, A. Rauf, A. N. Sabri, S. Riaz, and S. Naseem, "Size- and shape-dependent antibacterial studies of silver nanoparticles synthesized by wet chemical routes," *Nanomaterials*, vol. 6, no. 4, p. 74, 2016.

[65] T. Aigner, "Apoptosis, necrosis, or whatever: how to find out what really happens?," *The Journal of Pathology: A Journal of the Pathological Society of Great Britain and Ireland*, vol. 198, no. 1, pp. 1–4, 2002.

[66] C. Ciniglia, G. Pinto, C. Sansone, and A. Pollio, "Acridine orange/ethidium bromide double staining test: a simple in-vitro assay to detect apoptosis induced by phenolic compounds in plant cells," *Allelopathy Journal*, vol. 26, pp. 301–308, 2010.

[67] H. S. Kim, S. Kacew, and B. M. Lee, "In vitro chemopreventive effects of plant polysaccharides (Aloe barbadensis Miller, Lentinus edodes, Ganoderma lucidum and Coriolus versicolor)," *Carcinogenesis*, vol. 20, no. 8, pp. 1637–1640, 1999.

[68] M. M. Joseph, S. R. Aravind, S. K. George, S. Varghese, and T. T. Sreelekha, "A galactomannan polysaccharide from Punica granatum imparts in vitro and in vivo anticancer activity," *Carbohydrate Polymers*, vol. 98, pp. 1466–1475, 2013.

[69] M. Zhou, L. Yang, S. Yang, F. Zhao, L. Xu, and Q. Yong, "Isolation, characterization and in vitro anticancer activity of an aqueous galactomannan from the seed of Sesbania cannabina," *International Journal of Biological Macromolecules*, vol. 113, pp. 1241–1247, 2018.

[70] N. Ahmad and S. Sharma, "Green synthesis of silver nanoparticles using extracts of <i>Ananas comosus</i>," *Green and Sustainable Chemistry*, vol. 2, no. 4, pp. 141–147, 2012.

[71] P. Rauwel, S. Küünal, S. Ferdov, and E. Rauwel, "A review on the green synthesis of silver nanoparticles and their morphologies studied via TEM," *Advances in Materials Science and Engineering*, vol. 2015, 9 pages, 2015.

[72] B. Bahrami-Teimoori, Y. Nikparast, M. Hojatianfar, M. Akhlaghi, R. Ghorbani, and H. R. Pourianfar, "Characterisation and antifungal activity of silver nanoparticles biologically synthesised by Amaranthus retroflexus leaf extract," *Journal of Experimental Nanoscience*, vol. 12, pp. 129–139, 2017.

[73] C. Wang, X. Gao, Z. Chen, Y. Chen, and H. Chen, "Preparation, characterization and application of polysaccharide-based metallic nanoparticles: a review," *Polymers*, vol. 9, no. 12, p. 689, 2017.

[74] Y. Ma, C. Liu, D. Qu, Y. Chen, M. Huang, and Y. Liu, "Antibacterial evaluation of sliver nanoparticles synthesized by polysaccharides from Astragalus membranaceus roots," *Biomedicine & Pharmacotherapy*, vol. 89, pp. 351–357, 2017.

[75] Y. Matsumura, K. Yoshikata, S. I. Kunisaki, and T. Tsuchido, "Mode of bactericidal action of silver zeolite and its comparison with that of silver nitrate," *Applied and Environmental Microbiology*, vol. 69, no. 7, pp. 4278–4281, 2003.

[76] S. Rajeshkumar, "Chapter 10- Antifungal Impact of Nanoparticles Against Different Plant Pathogenic Fungi," in *Nanomaterials in Plants, Algae and Microorganisms*, D. K. Tripathi, P. Ahmad, S. Sharma, D. K. Chauhan, and N. K. Dubey, Eds., pp. 197–217, Academic Press, 2019.

[77] T. C. Dakal, A. Kumar, R. S. Majumdar, and V. Yadav, "Mechanistic basis of antimicrobial actions of silver nanoparticles," *Frontiers in Microbiology*, vol. 7, p. doi:10.3389/fmicb.2016.01831, 2016.

[78] V. Gopinath and P. Velusamy, "Extracellular biosynthesis of silver nanoparticles using Bacillus sp. GP-23 and evaluation of their antifungal activity towards Fusarium oxysporum," *Spectrochimica Acta Part A: Molecular and Biomolecular Spectroscopy*, vol. 106, pp. 170–174, 2013.

[79] C. Krishnaraj, R. Ramachandran, K. Mohan, and P. T. Kalaichelvan, "Optimization for rapid synthesis of silver nanoparticles and its effect on phytopathogenic fungi," *Spectrochimica Acta Part A: Molecular and Biomolecular Spectroscopy*, vol. 93, pp. 95–99, 2012.

[80] M. Thenmozhi, K. Kannabiran, R. Kumar, and V. Gopiesh Khanna, "Antifungal activity of Streptomyces sp. VITSTK7 and its synthesized Ag2O/Ag nanoparticles against medically important Aspergillus pathogens," *Journal de Mycologie Médicale*, vol. 23, pp. 97–103, 2013.

[81] R. J. B. Pinto, A. Almeida, S. C. M. Fernandes et al., "Antifungal activity of transparent nanocomposite thin films of pullulan and silver against Aspergillus niger," *Colloids and Surfaces B: Biointerfaces*, vol. 103, pp. 143–148, 2013.

[82] E. Elsherbiny, N. Safwat, and M. Elaasser, "Fungitoxicity of organic extracts of Ocimum basilicum on growth and morphogenesis of Bipolaris species (teleomorph Cochliobolus)," *Journal of Applied Microbiology*, vol. 123, no. 4, pp. 841–852, 2017.

[83] J. Worapattamasri, N. Ninsuwan, S. Chuenchit, and V. Petcharat, "Anamorphs of Cochliobolus on disease plants in Southern Thailand," *Journal of Agricultural Technology*, vol. 5, pp. 143–155, 2009.

[84] K. E. Kaylegian, J. M. Lynch, J. R. Fleming, and D. M. Barbano, "Lipolysis and proteolysis of modified and producer milks used for calibration of mid-infrared milk analyzers 1," *Journal of Dairy Science*, vol. 90, pp. 602–615, 2007.

[85] P. Zajác, S. Zubrická, J. Čapla, L. Zeleňáková, R. Židek, and J. Čurlej, "Effect of preservatives on milk composition determination," *International Dairy Journal*, vol. 61, pp. 239–244, 2016.